Patterned growth on GaAs (311)A substrates: Engineering of growth selectivity for lateral semiconductor nanostructures

Jörg Fricke,[a] Richard Nötzel,[b] Uwe Jahn, Zhichuan Niu,[c] Hans-Peter Schönherr, Manfred Ramsteiner, and Klaus H. Ploog
Paul-Drude-Institute for Solid State Electronics, Hausvogteiplatz 5-7, D-10117 Berlin, Germany

(Received 23 March 1999; accepted for publication 2 June 1999)

The growth selectivity on patterned GaAs (311)*A* substrates differs qualitatively from that on low-index (100) and (111) substrates. During molecular beam epitaxy of (Al,Ga)As, [01-1] oriented mesa stripes develop a fast growing convex sidewall. A continuous transition occurs towards the slow growing concave sidewall upon turning the mesa along the perpendicular [-233] direction without breaking up the growth front into microfacets. This allows their systematic combination at the corner or edge of intersecting mesa stripes appropriately inclined from [01-1] among which we highlight those involving fast growing sidewalls. The scenario, which is unique for patterned GaAs (311)*A* substrates, offers a novel degree of flexibility for the design of lateral functional semiconductor nanostructures. © *1999 American Institute of Physics.* [S0021-8979(99)06617-7]

I. INTRODUCTION

Epitaxial growth on patterned substrates is the focus of many research groups for the formation of low-dimensional structures, i.e., quantum wires and quantum dots, as well as for basic growth studies.[1–7] The growth of V-groove[1,2] and ridge-type structures[3–7] has been most widely investigated on patterned low-index [100] and [111] oriented substrates. It is based on the formation of slow growing side facets due to the migration of adatoms away from the sidewalls to the mesa top or bottom which produces a concave surface profile at the corners. We have recently found a qualitatively different growth mechanism in the molecular beam epitaxy (MBE) of (Al,Ga)As on patterned high-index substrates. [01-1] oriented mesa stripes on patterned GaAs (311)*A* substrates develop on one side, in the sector towards the next (100) plane, a very smooth fast growing convex sidewall without any faceting.[8] The formation of this sidewall relies on the migration of adatoms from the mesa top and mesa bottom to the sidewall which is opposite in direction to that on patterned low-index substrates. The opposite sidewall as well as the perpendicular mesa stripes along [-233] develop slow growing side facets. For shallow mesa heights the formation of the fast growing sidewall has resulted in quantum wire and quantum dot structures with excellent structural and electronic properties.[9,10]

A detailed study of the dependence of growth selectivity on the mesa misalignment and sidewall slope after etching has revealed a continuous decrease of the growth selectivity for wet chemically etched sidewalls with about 50° slope upon misalignment from the [01-1] direction that develops smoothly from the fast to the slow growing sidewall along [-233] for misalignment larger than 50°.[11] For reactive ion (RI) etched vertical sidewalls along [01-1], however, the growth terminates close to the next (111) facet inclined about 80° while the evolution of the fast growing sidewall returns for misaligned mesa stripes. It is important that the transition from the fast growing to the slow growing sidewall occurs without the growth front breaking up into microfacets which is commonly encountered on low-index substrates.[12] The surface remains as smooth as that in planar areas. This allows combination of sidewalls with different character (fast or slow growing) and/or varied growth selectivity at the corners or edges of intersecting mesa stripes appropriately inclined from [01-1]. The systematic study on the various possible combinations of growth selectivity presented here supplements the recently reported growth phenomena leading to coupled wire-dot arrays[11] and triangular-shaped dot-like structures.[13] Cathodoluminescence imaging evidences the formation of novel isolated dot-like structures at the edge of intersecting fast and slow growing sidewalls and a dense matrix of dot stuctures in the fast growing corners of triangular hole patterned substrates. This reveals a great flexibility for the formation of functional lateral semiconductor nanostructures which is unique for patterned GaAs (311)*A* substrates.

II. EXPERIMENTAL PROCEDURE

Standard optical lithography, using an AZ5214 photoresist, was used for pattern definition. The pattern transfer into the GaAs substrates was then performed by either wet chemical etching in H_2SO_4:H_2O_2:H_2O (1:8:40) or by RI etching using a Cl_2/N_2 plasma in a standard parallel-plate reactor that produced a smooth surface morphology with low damage. The etch depth was 500 nm for the growth studies and several 10 nm for nanostructure formation. After etching the samples were cleaned in concentrated H_2SO_4 and rinsed in de-ionized water. The native oxide was removed in the MBE preparation chamber using atomic hydrogen irradiation before loading the samples into the growth chamber. On the

[a]Now at: Ferdinand-Braun-Institute, Rudower Chaussee 5, 12489 Berlin.
[b]Corresponding author.
[c]Now at: Institute of Semiconductors, P.O. Box 912, Beijing 100083.

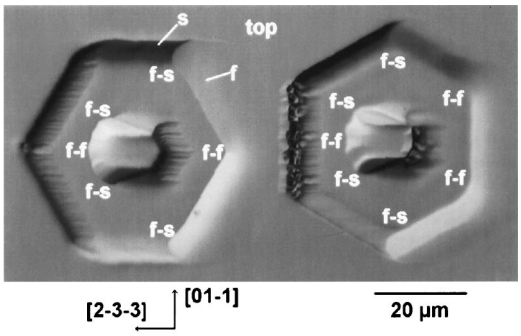

FIG. 1. Surface image by optical microscopy of the 500 nm deep hexagonal hole and mesa patterns after overgrowth. Combinations of fast (*f*) and slow (*s*) growing sidewalls in the corners of the holes and at the edges of the mesas are indicated.

deep mesa etched substrates the grown layer sequence comprised a 1–2 μm thick GaAs buffer to develop the surface morphology with several $Al_{0.5}Ga_{0.5}As$ marker layers inserted. This was followed by a 3–6 nm thick quantum-well layer embedded between 10 nm thick $Al_{0.5}Ga_{0.5}As$ lower and upper barrier layers and finally capped with 20 nm GaAs. On the shallow mesa etched substrates the GaAs buffer layer was 50 nm thick followed by a 50 nm $Al_{0.5}Ga_{0.5}As/2-3$ nm GaAs/50 nm $Al_{0.5}Ga_{0.5}As$ quantum-well layer capped with 20 nm of GaAs. The growth temperature was 620 °C, the GaAs and $Al_{0.5}Ga_{0.5}As$ growth rates were 0.5 and 1 μm/h, respectively, and the group V-III flux ratio was about 5. These growth conditions were chosen as the optimum ones on GaAs (311)*A* substrates with regard to crystal quality and surface morphology. To avoid any shadowing effects the substrates were rotated 6 rpm during growth. The growth evolution was deduced from optical microscopy, scanning electron microscopy (SEM), and atomic force microscopy (AFM) of the sample surface which was complemented by spectrally and spatially resolved cathodoluminescence (CL) and microphotoluminescence (PL) spectroscopy revealing the corresponding thickness variation of the quantum-well layer and lateral nanostructure formation.

III. GROWTH STUDIES

The fundamental combinations of fast and slow growing sidewalls in the corner or at the edge of two intersecting sidewalls are realized for the two hexagonal hole patterns with hexagonal mesas of the same inside shape which are rotated 30° relative to each other (Fig. 1). The respective combinations are indicated by ''*f*'' for the fast growing and ''*s*'' for the slow growing sidewall. The reduction of the growth selectivity of the fast growing sidewall upon mesa rotation and the transition to the slow growing sidewall along [-233] leading to *f-f* and *f-s* combinations is evident together with preservation of the very smooth surface morphology. The opposite sidewalls leading to *s-s* combinations, however, show pronounced roughening and faceting along [-233]. This has been related to the microscopic surface corrugation of GaAs (311)*A* planes along [-233] that destabilize the growth of slow growing side facets along [01-1], and at the same time stabilize the formation of slow growing side facets

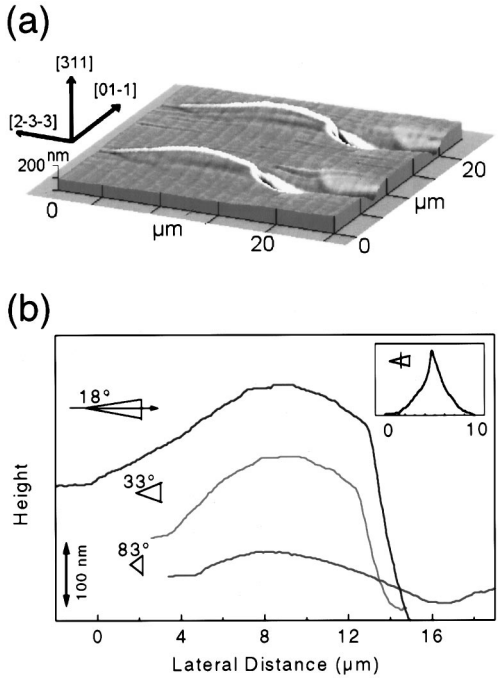

FIG. 2. (a) AFM image of 500 nm high triangular mesas with an acute angle of 18° pointing towards the fast growing sidewall after overgrowth. (b) AFM line scans along the edge of triangular mesas with acute angles of 18°, 33°, and 83°. Inset: Perpendicular line scan across the ridge.

along [-233].[14] The smoothness of the fast growing sidewalls is related to the absence of any faceting at all, due to the nature of their formation.

For the *f-s* combination in the corners of the hexagonal holes as well as at the edges of the inner mesas, a clear superposition of the ridge formation due to migration of adatoms from the slow growing sidewall to the mesa top with the convex fast growing sidewall occurs. At the corner, the ridge of the slow growing sidewall continues over the intersection of the fast and slow growing sidewalls on the mesa top in the direction opposite to that of the fast growing sidewall. A very uniform, freely developing part of the ridge nucleates at this intersection. This is the starting point for the formation of triangular-shaped dot-like structures on substrates patterned with square- and triangular-shaped hole arrays which evolve between neighboring holes on the original substrate surface.[13] The *f-s* combination at the edges of the mesas produces the ridge of the slow growing sidewall following the convex curvature of the fast growing sidewall which results in additional accumulation of material along the intersection. The *f-f* combination in the corners and at the edges shows a smooth transition between the sidewalls and has an overall convex surface profile.

Two situations not covered by the hexagonal pattern in Fig. 1 are edges or corners pointing towards the fast growing sidewall which are bound on both sides by slow growing sidewalls (*s-f-s* combination), i.e., mesas or holes with edges and corners with small acute angles along $\langle 233 \rangle$. Figure 2(a) shows the AFM image of such a triangular mesa with an 18° acute edge angle after overgrowth. In contrast to the *f-f* combination in Fig. 1, the *s-f-s* combination with slow growing sidewalls forming the nominally fast growing edge results in

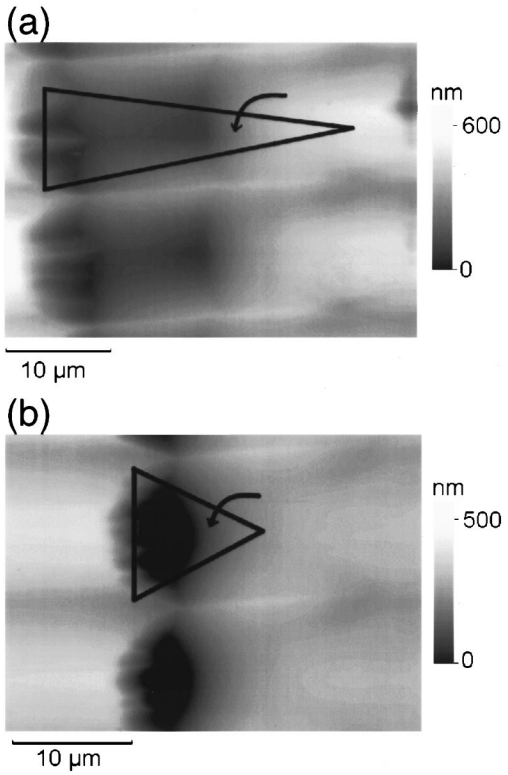

FIG. 3. AFM image of 500 nm deep triangular holes with fast growing corners for (a) 20° and (b) 80° acute angles after overgrowth. The as-etched shape of the triangular holes is indicated. The arrows indicate the preferential migration of adatoms into the fast growing corners.

a concave surface profile of the edge along [2-3-3], which is that of a slow growing sidewall. Indeed, a clear changeover from the fast growing shape of the edge to the slow growing one is observed upon reducing the acute angle which coincides with the transition from fast to slow growing sidewalls of the triangle [see the AFM line scans in Fig. 2(b) along [-233] over the edge for triangular mesas with 83°, 33°, and 18° acute angles]. Hence, the superposition of two slow growing sidewalls forces the edge to convert from a convex fast growing shape to a concave slow growing one of the adjacent sidewalls which form a sharp ridge along the edge [see the inset of Fig. 2 (b)] thereby suppressing the adatom migration towards it.

On the other hand, the convex curvature of the fast growing sidewall is maintained in the corners, independent of the angle, i.e., the character of the adjacent sidewalls. Figures 3(a) and 3(b) show triangular holes with acute angles of 20° and 80°. Sketches are included to show the original shape of the holes before overgrowth. The evolution of the fast growing corners in Figs. 3(a) and 3(b), however is different. For the acute angle of 20°, the corner reveals fast filling and straight propagation of the fast growing sidewall. This might be related to the slow growing character of the sidewalls that supports filling of the corner due to migration of adatoms down the side facets and into the hole. In contrast, the corner bound by two fast growing sidewalls in Fig. 3(b) remains, but it becomes more round due to faster propagation with the larger growth selectivity in the corner compared to the smaller propagation at the sidewalls with reduced growth selectivity related to their misalignment from [01-1].

By generalizing the appearance of the rich variety of surface patterns originating from the combination of sidewalls with different character and/or varied growth selectivity it can be concluded from the results presented that the complex growth behavior relies on straightforward superposition of growth selectivity in terms of the amount and the direction of the migrating adatoms. This underscores the significance of the two possible growth mechanisms on patterned substrates, i.e., the formation of the slow and, in particular, the fast growing sidewall simultaneously occurring on patterned GaAs (311)*A* substrates.

IV. NANOSTRUCTURE FORMATION

All combinations of fast and slow growing sidewalls discussed above result in distinct thickness modulations of the inserted quantum well imaged by CL mapping which in general support the growth selectivity deduced from the surface morphology. In view of the nanostructure formation, i.e., spatial definition and magnitude, two cases, the *f-s* combination at the edges and the *f-f* combination in the corners, prove most promising. The growth selectivity of the *s-f-s* (Fig. 2) and also the *f-f* combination at the edges is negligible compared to the adjacent parts for both deep and shallow etched mesas which can be understood from its easy reduction and conversion into the slow growing shape for the *s-f-s* case.

To exploit the *f-s* combination at the edge (and simultaneously in the corner), a periodic zigzag pattern, 60° off the [01-1] direction [see Fig. 4(a)] was fabricated by RI etching with the 500 nm deep fast and slow growing sidewalls misaligned about 30° from the [01-1] and [-233] directions, respectively. RI etching was used to achieve good definition of the corners and edges. The 30° misalignment, then, provides the highest growth selectivity for vertical fast growing sidewalls.[11] The SEM image in Fig. 4(b) reveals the typical *f-s* combination characterized by the ridge following the convex profile, indicative for the formation of dot-like nanostructures at the mesa bottom. This is confirmed by the μ-PL spectrum and CL image in the inset of Fig. 5 which show an array of dot-like emission centers at the bottom edges of the zigzag pattern. The linewidth of the PL emission, centered at 1.564 eV, is 8.5 meV and it is shifted 200 meV to lower energy relative to the quantum-well luminescence (Qwell) at 1.791 eV in unpatterned areas. The growth selectivity of the fast growing sidewall parts in between in the adjacent corners is strongly suppressed due to the nearby ridge formation with peak emission energy close to that of the quantum well. The dot-like emission can, however, depending on the precise orientation of the mesa sidewalls and/or layer thickness, easily extend along the ridge leading to a comma shaped CL image. Moreover, the growth selectivity is strongly reduced for shallow mesa height due to planarization of the ridge.

The *f-f* combination in corners can generate lateral nanostructures at shallow mesas in the extension of the formation of [01-1] oriented sidewall quantum wires. For this, the periodic zigzag pattern is aligned along [01-1] [see the schematic in Fig. 6(a)]. Figure 6(b) shows the shallow mesa side-

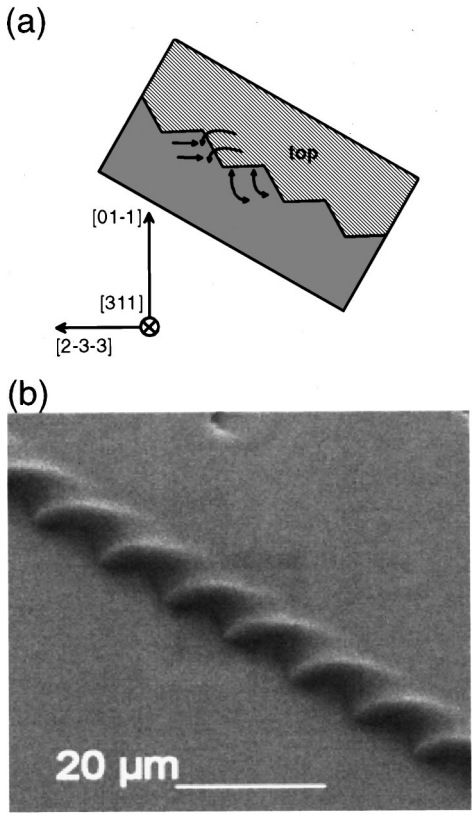

FIG. 4. (a) Schematic of the zigzag pattern combining fast and slow growing sidewalls. The arrows indicate the direction of adatom migration. (b) SEM image of the 500 nm high mesa structure after overgrowth.

wall, 20 nm in height, after overgrowth with the larger growth selectivity in the corner compared to that at the adjacent mesa sidewalls similar to the deep hole in Fig. 3(b). This structure has been utilized previously for the formation of coupled wire-dot arrays connecting a dot structure in the corner with lower band gap energy (higher growth selectivity) to the wire at the sidewall with higher band gap energy

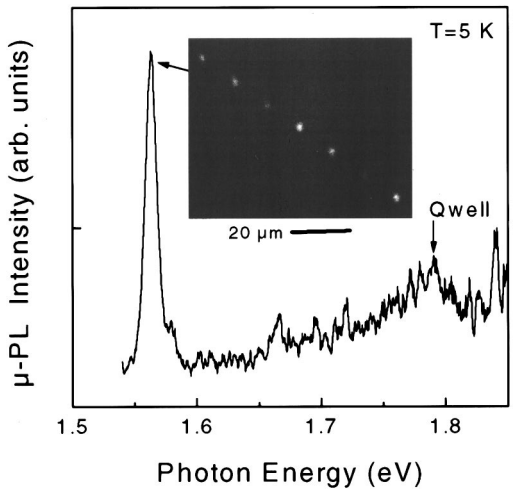

FIG. 5. μ-PL spectrum taken at 5 K from the bottom edge of the zigzag structure depicted in Fig. 4(b). Qwell denotes the PL peak energy of the 2 nm thick quantum well in unpatterned, planar areas at 1.791 eV. Inset: CL image of the dot-like emission pattern from the bottom edges detected at the μ-PL peak position at 1.564 eV.

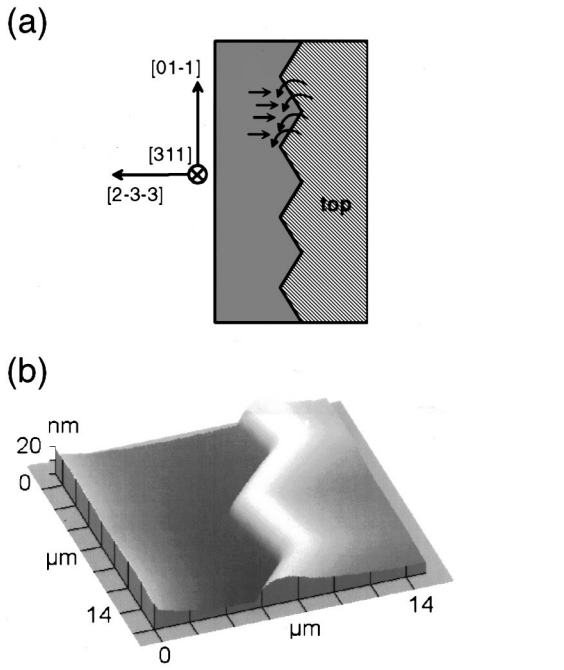

FIG. 6. (a) Schematic of the zigzag pattern combining two fast growing sidewalls with reduced growth selectivity. The arrows indicate the direction of adatom migration. (b) AFM image of the 20 nm high mesa structure after overgrowth.

(smaller growth selectivity).[11] Therefore, we concentrate here on the formation of a dense matrix of isolated dot-like structures formed at the fast growing corners of a two-dimensional array of triangular holes.

Holes with a side length of 1 μm and distance of 500 nm were fabricated by electron beam lithography and RI etching to a depth of 50 nm. The AFM image of the sample surface after overgrowth [Fig. 7(a)] reveals the fast growing sidewall at the corners developing into the triangle sidewalls with smaller growth selectivity, maintaining the triangular shape. The corresponding area averaged CL spectrum of the 3 nm thick quantum-well layer in Fig. 7(b) is composed of two lines at 1.703 and 1.598 eV with a 8 meV linewidth which originate from the almost planar parts between the holes on the substrate surface (the peak energy shift with respect to the quantum-well emission in unpatterned areas is smaller than 3 meV) and from the fast growing corners inside the holes, respectively. This is confirmed by the CL images detected at the corresponding CL peak energies shown in Figs. 7(c) and 7(d). No contrast is visible from the triangular-shaped tips between the holes on the substrate surface or from the opposite rough sidewalls in the holes compared to larger structures[13] suggesting here also smearing out of the ridge-type structure and of the rough slow growing sidewalls for shallow mesa height and small pattern size. The triangular shape of the CL emission of the fast growing corners in the holes is attributed to diffusion of photogenerated carriers from the thinner sidewalls of the holes to the thicker corner where they recombine; however, a smooth transition in thickness from the sidewalls to the corners dominating the growth in the small holes cannot be excluded.

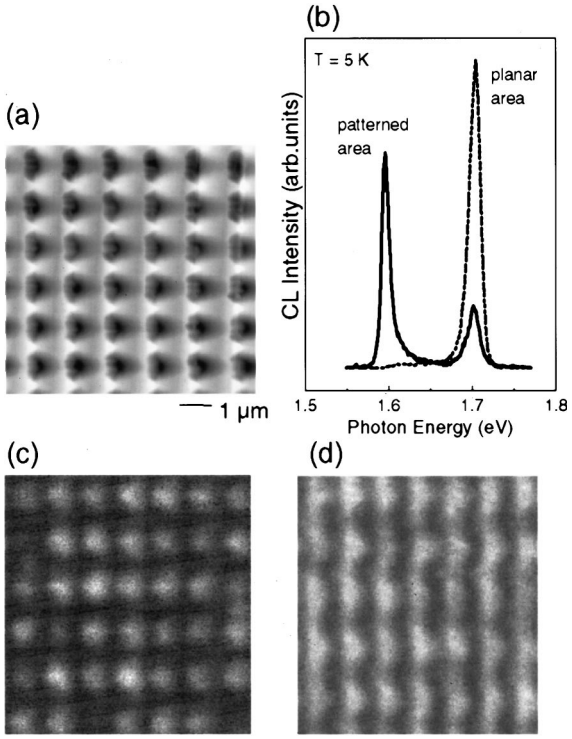

FIG. 7. (a) AFM image of the dense two-dimensional hole array with fast growing corners after overgrowth. The holes are 50 nm deep. (b) Area averaged CL spectrum taken at 5 K from the pattern (solid line). The dashed line is the CL spectrum of the 3 nm thick quantum well in unpatterned, planar areas. (c) and (d) are the corresponding CL images detected at the CL peak positions at 1.703 and 1.598 eV of the areas between the holes and the corners, respectively.

V. CONCLUSION

In conclusion, we have systematically investigated the superposition of growth selectivity on patterned GaAs (311)*A* substrates at the intersection of fast and slow growing mesa sidewalls by molecular beam epitaxy. Appropriate pattern design allows combinations of fast growing and slow growing mesa sidewalls with different growth selectivity controlled by the mesa misalignment with respect to [01-1]. The resulting surface morphologies can be understood by the straightforward addition of growth selectivity in terms of the amount and the direction of migrating adatoms depending on the character of the constituent sidewalls. This study presents the basis for the formation of novel lateral semiconductor nanostructures on patterned GaAs (311)*A* substrates and supplements the recently reported growth phenomena leading to the formation of coupled wire-dot arrays and triangular-shaped dot-like structures. It provides a universal tool for quantum-well tailoring which has been exploited in the present work for the case of isolated dot arrays at the intersection of a fast with a slow growing mesa sidewall and of a dense two-dimensional matrix of isolated dot-like structures at the fast growing corners of triangular-shaped holes. More complex surface patterns can be envisioned for the direct epitaxial growth of novel lateral functional semiconductor nanostructures.

ACKNOWLEDGMENTS

The authors thank E. Wiebicke for sample preparation. Part of this work was supported by the Bundesministerium für Bildung Wissenschaft Forschung und Technologie and by NEDO NTDP-98 project.

[1] E. Kapon, D. M. Hwang, and R. Bhat, Phys. Rev. Lett. **63**, 430 (1989).
[2] X. L. Wang, M. Ogura, and H. Matsuhata, J. Cryst. Growth **171**, 341 (1997).
[3] M. Walther, T. Röhr, G. Böhm, G. Tränkle, and G. Weimann, J. Cryst. Growth **127**, 1045 (1993).
[4] K. C. Rajkumar, A. Madhukar, K. Rammohan, D. H. Rich, P. Chen, and L. Chen, Appl. Phys. Lett. **63**, 2905 (1993).
[5] S. Tsukamoto, Y. Nagamune, M. Nishioka, and Y. Arakawa, Appl. Phys. Lett. **63**, 355 (1993).
[6] S. Koshiba, *et al.* Appl. Phys. Lett. **64**, 363 (1994).
[7] H. Fujikura and H. Hasegawa, J. Cryst. Growth **150**, 327 (1995).
[8] R. Nötzel, J. Menniger, M. Ramsteiner, A. Ruiz, H. P. Schönherr, and K. H. Ploog, Appl. Phys. Lett. **68**, 1132 (1996).
[9] A. Richter, G. Behme, M. Süptitz, Ch. Lienau, T. Elsässer, M. Ramsteiner, R. Nötzel, and K. H. Ploog, Phys. Rev. Lett. **79**, 2145 (1997).
[10] R. Nötzel, Z. C. Niu, M. Ramsteiner, H. P. Schönherr, A. Trampert, L. Däweritz, and K. H. Ploog, Nature (London) **392**, 56 (1998).
[11] J. Fricke, R. Nötzel, U. Jahn, H. P. Schönherr, L. Däweritz, and K. H. Ploog, J. Appl. Phys. **85**, 3576 (1999).
[12] M. Kihara, H. Fujikura, and H. Hasegawa, Appl. Surf. Sci. **117/118**, 695 (1997).
[13] Z. C. Niu, R. Nötzel, U. Jahn, H. P. Schönherr, J. Fricke, and K. H. Ploog, J. Electron. Mater. **28**, 1 (1999).
[14] R. Nötzel, J. Menniger, M. Ramsteiner, A. Trampert, H. P. Schönherr, L. Däweritz, and K. H. Ploog, J. Cryst. Growth **175/176**, 1114 (1997).